

Quantum computations of relativistic and many-body effects in atomic and molecular systems based on variational algorithms

Bhanu Pratap Das,

Centre for Quantum Engineering, Research and Education TCG CREST, Kolkata

Dept. of Physics, Tokyo Institute of Technology, Tokyo

RPMBT22, Tsukuba, 25 September, 2024



Collaborators: Akhil P. Singh, Palak Chawla, Shweta, K. R. Swain, Tushti Patel, Renu Bala, Disha Shetty, Sudhindu B. Mandal, Jordi Riu, Jan Nogu e, Akitada Sakurai, Nanako Shitara, V.S. Prasanna, Kenji Sugisaki, Yasunobu Nakamura

Vikrant Kumar, Nishanth Baskaran, Debashis Mukherjee, Kenneth Dyll

Outline

- Variational Quantum Eigensolver (VQE):
 - Brief introduction to VQE.
 - Applications to ground state energies and hyperfine interactions in atoms.
 - Dipole moments of molecules.
- Quantum Annealer Eigensolver (QAE):
 - Brief introduction to QAE.
 - Applications to fine structure splitting in atoms.

The focus of both variational algorithms in this talk will be on quantum computations of relativistic and many-body effects.

Digital quantum computing

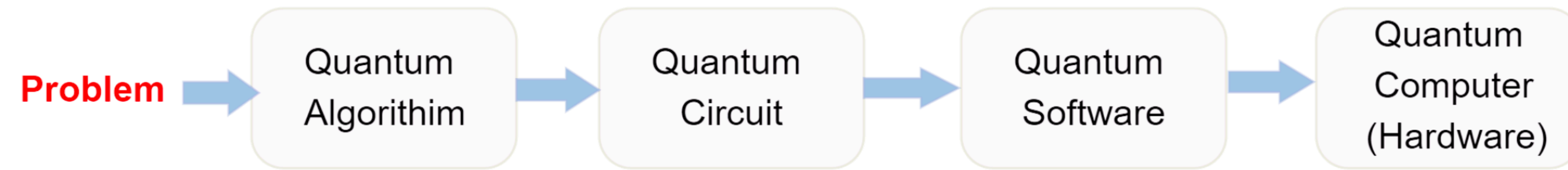


Figure: Flowchart for Quantum Computation

- **Qubits:** Quantum states $a|0\rangle + b|1\rangle$.
- **Quantum gates:** Unitary operators. $R_X(\theta) = e^{-i\frac{\theta}{2}X}$, $R_Y(\theta) = e^{-i\frac{\theta}{2}Y}$, and $R_Z(\theta) = e^{-i\frac{\theta}{2}Z}$: examples of 1-qubit gates. *CNOT*: an example of a 2-qubit gate.
- Quantum computation using **quantum circuits** (qubits and quantum gates):

$$|00\rangle \xrightarrow{R_X(\theta)} \cos\left(\frac{\theta}{2}\right)|00\rangle - i\sin\left(\frac{\theta}{2}\right)|10\rangle \xrightarrow{CNOT} \cos\left(\frac{\theta}{2}\right)|00\rangle - i\sin\left(\frac{\theta}{2}\right)|11\rangle.$$

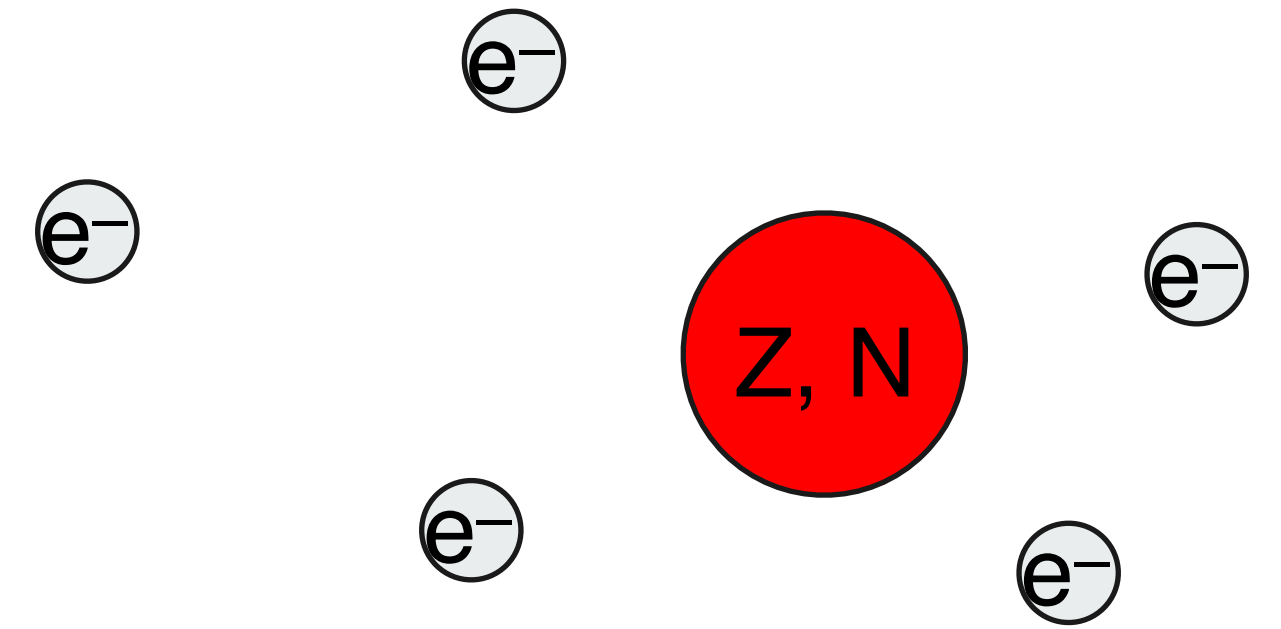


- In our quantum computation, we use **layers of rotations and CNOT gates**.

Relativistic Effects in Atomic Systems

Non-Relativistic Hamiltonian

$$H_{nr} = \sum_i \left(\frac{p_i^2}{2m} + V_{nuc} \right) + \sum_{i<j} \frac{e^2}{r_{ij}}$$



For large Z, velocities of electrons increase and they must be treated relativistically

Relativistic Hamiltonian

$$H_{DC} = \sum_i \left(c\alpha_i \cdot p_i + \beta_i mc^2 + V_{nuc} \right) + \sum_{i<j} \frac{e^2}{r_{ij}} \quad : \text{Dirac-Coulomb Hamiltonian}$$

Leading order correction to the Coulomb interaction is the **Breit interaction**

$$H_B = -\frac{e^2}{2} \sum_{i<j} \left(\frac{\alpha_i \cdot \alpha_j}{r_{ij}} + \frac{(\alpha_i \cdot r_{ij})(\alpha_i \cdot r_{ij})}{r_{ij}^3} \right)$$

α and β are (4x4) matrices. Other relativistic corrections are generally less important.

Hyperfine structure constant

- The **hyperfine Hamiltonian** is given by $H_{hf} = \vec{j}_e \cdot \vec{A}_N$.
- The quantity can be represented as an **effective Hamiltonian**: $H_{hf}^{eff} = \mathcal{A} \vec{I} \cdot \vec{J}$.
- $$\mathcal{A} = \frac{1}{J} \mu_N g_I \langle JJ | \sum_i \frac{(\vec{r}_i \times \vec{\alpha}_i)_Z}{r_i^3} | JJ \rangle.$$
- \mathcal{A} is often a difficult quantity to evaluate, since it is determined by a complex interplay of several electron correlation effects, unlike the energy.
- Its computation requires accurate single particle wave functions in the nuclear region, and hence computing \mathcal{A} is a sensitive test of relativistic and correlation effects in atoms and molecules.

VQE algorithm

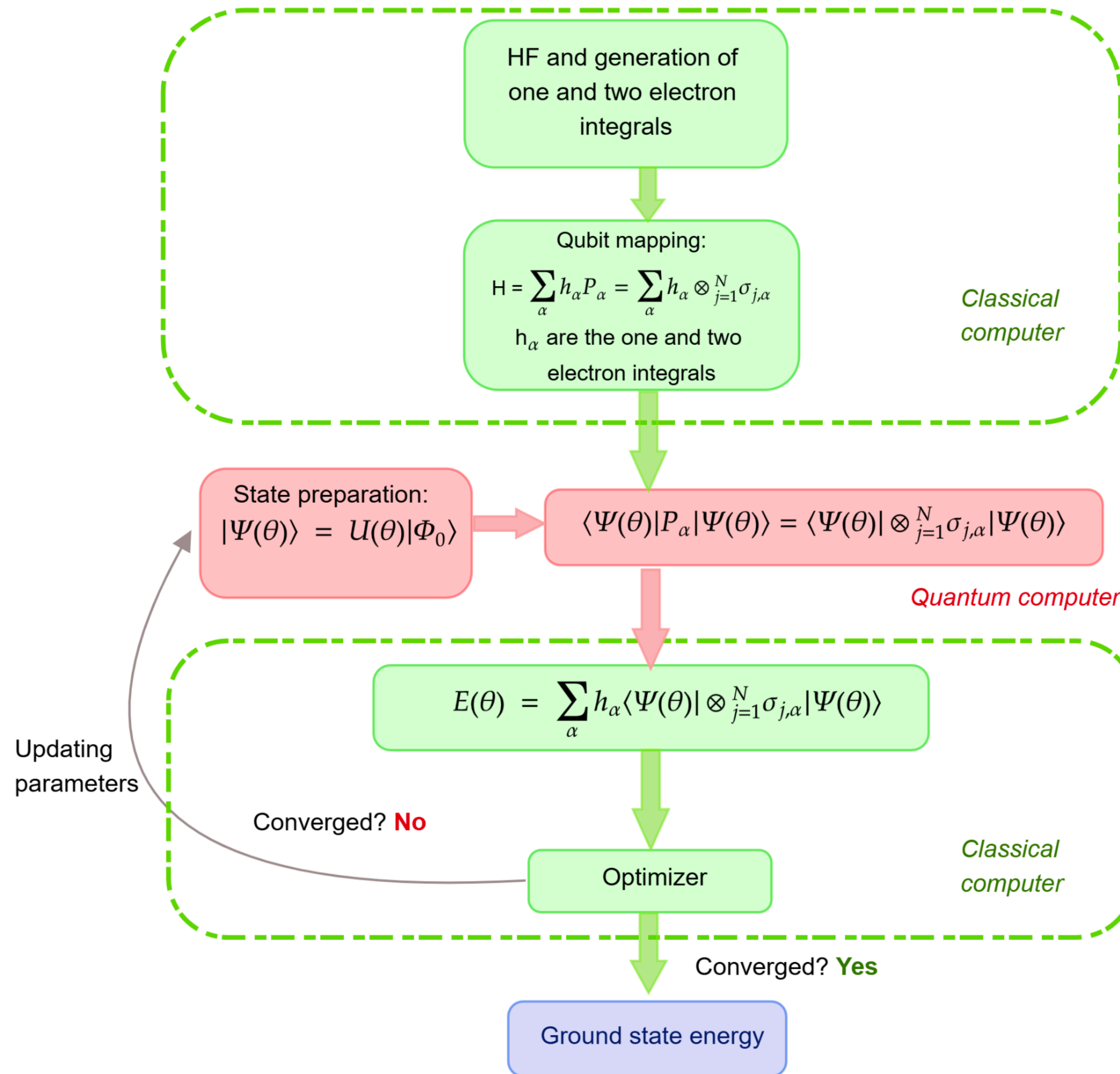
VQE

Introduction

- Hybrid (classical-quantum) algorithm to calculate ground state energies and other properties of quantum many-body systems. It is suitable for NISQ computers (50-100 qubits).
- $|\Phi_0\rangle$ can be written in terms of orbitals, where each orbital is $|\phi_i\rangle = |n_i l_i m_{l,i} s_i m_{s,i}\rangle$ or $|n_i l_i s_i j_i m_i\rangle$ is a qubit. In qubit representation,

$$|\Phi_0\rangle = \underbrace{|1\rangle \otimes \dots \otimes |1\rangle}_{\text{Occupied}} \otimes \underbrace{|0\rangle \otimes \dots \otimes |0\rangle}_{\text{Unoccupied}}$$
- The variational principle is used to find the ground state energy of a system:
 $E(\theta) = \langle \Psi(\theta) | H | \Psi(\theta) \rangle$; $|\Psi(\theta)\rangle = U(\theta) |\Phi_0\rangle$. Minimise $E(\theta) = \langle \Phi_0 | U(\theta)^\dagger H U(\theta) | \Phi_0 \rangle$ by varying till convergence is reached. Expectation value: $\langle \Phi_0 | U(\theta)^\dagger A U(\theta) | \Phi_0 \rangle$;
 $A = \sum_{pq} A_{pq} a_p^\dagger a_q$; A_{pq} (one particle matrix element) from classical computer.
- The choice of $U(\theta)$ is crucial for obtaining an accurate value for energy and other properties.
- A physically motivated ansatz for $U(\theta)$ is based on **unitary coupled cluster(UCC)** method, where $U(\theta = t) = e^{T-t^\dagger}$. Where T and t is cluster operator and amplitudes.
 $T = T_1 + T_2 \dots = \sum_{ia} t_i^a a_a^\dagger a_i + \sum_{ijab} t_{ij}^{ab} a_a^\dagger a_b^\dagger a_j a_i + \dots$ (A Peruzzo et al, Nature Communications 2014)
 Another choice is the **hardware efficient ansatz(HEA)**- e.g
 $U(\theta) = \prod [R(\theta)] \times CNOT$ (A Kandala et al, Nature 2017)

VQE Flowchart



VQE algorithm for relativistic calculations of ground state energies and hyperfine structure constants

- Hyperfine structure constants computation for neutral Li and highly charged isoelectronic systems: Li-like Sc, Li-like Pr, and Li-like Bi.
- Four qubit computations on superconducting qubit hardware at RIKEN (Nakamura lab).
- Choice of hardware efficient ansatz: $R_X(\pi/2) - R_Z(\theta) - R_X(\pi/2) - CNOT$ type. Linear entanglement strategy. Depth of one.
- Benchmarked with all-electron calculations in the complete Hilbert subspace that was considered.
- The major challenge: the same ansatz needs to capture dissimilar correlation effects involved in both properties.

'Exp' refers to computation on a quantum computer.

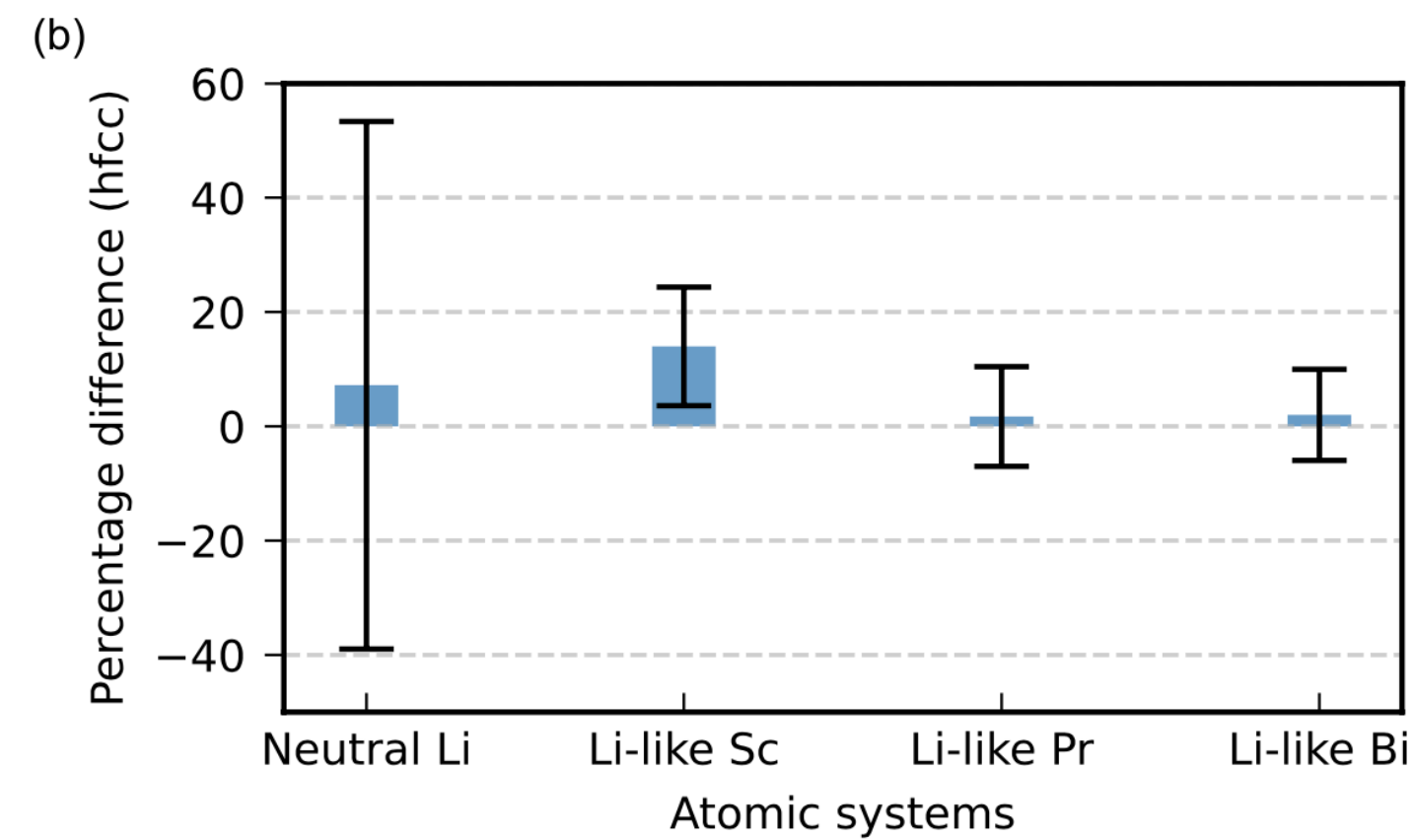
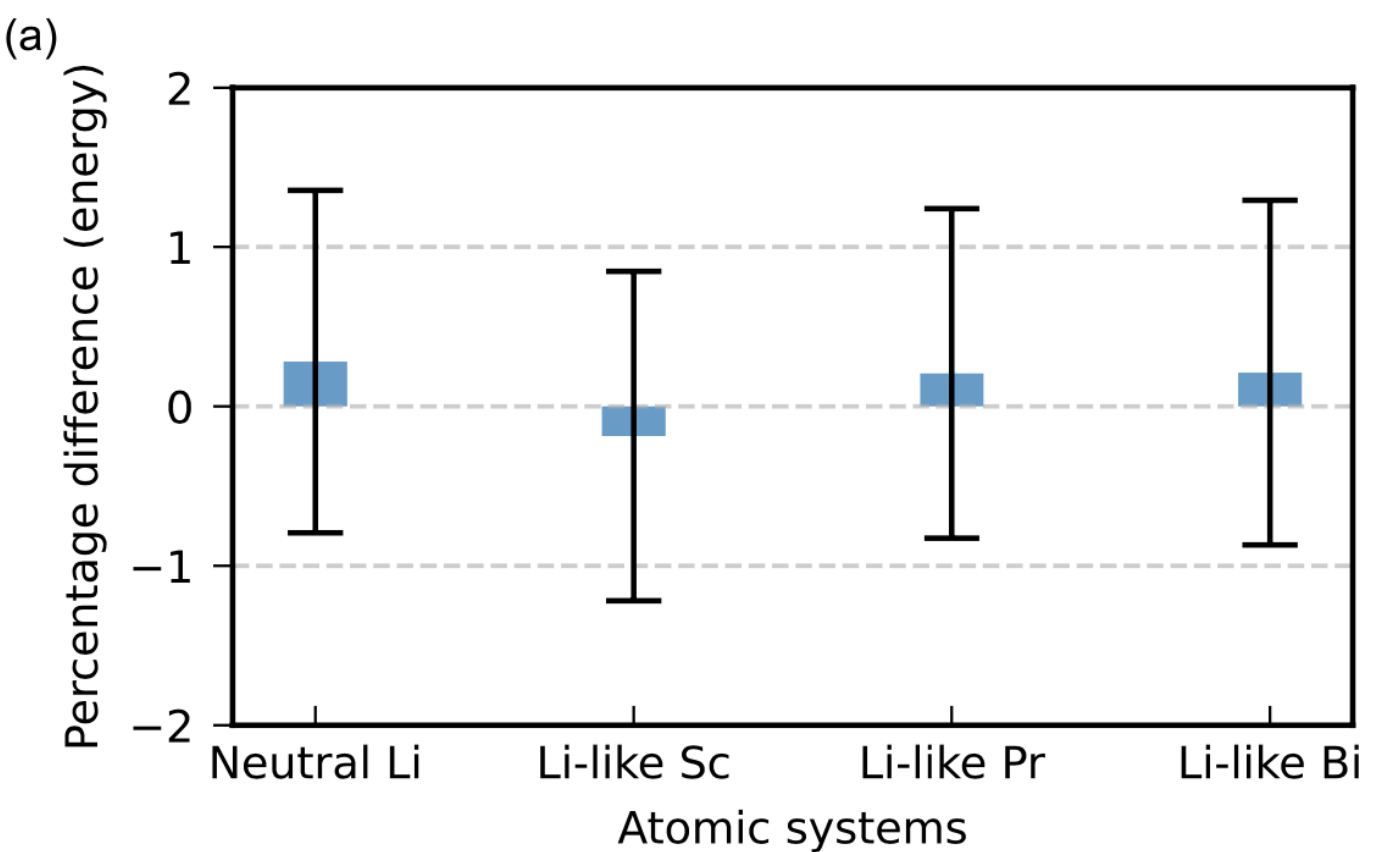
$$\mathcal{A}^{exp} = \langle H_{hfs}^q \rangle = \sum_l w_l^{hfs} \langle P_l \rangle^{exp}$$

Evaluated on a classical computer. \nearrow \nwarrow Evaluated on a quantum computer.

Error can occur from both these sources.

$$\Delta_r^{\mathcal{A}} = \frac{|\mathcal{A}^{exp} - \mathcal{A}^{CAS-CI}|}{|\mathcal{A}^{CAS-CI}|}$$

\nwarrow Assume this is 'perfect'.



State-of-the-art:

- Hardware efficient ansatz: Kandala et al (Nature 2017): best precision is 1.6 mHa for H2 in its equilibrium bond length.
- UCC Ansatz: Guo et al (Nature Physics 2024): Best precision is ~0.1 mHa for H2 in its equilibrium bond length.

VQE algorithm for relativistic calculations of molecular electric dipole moments

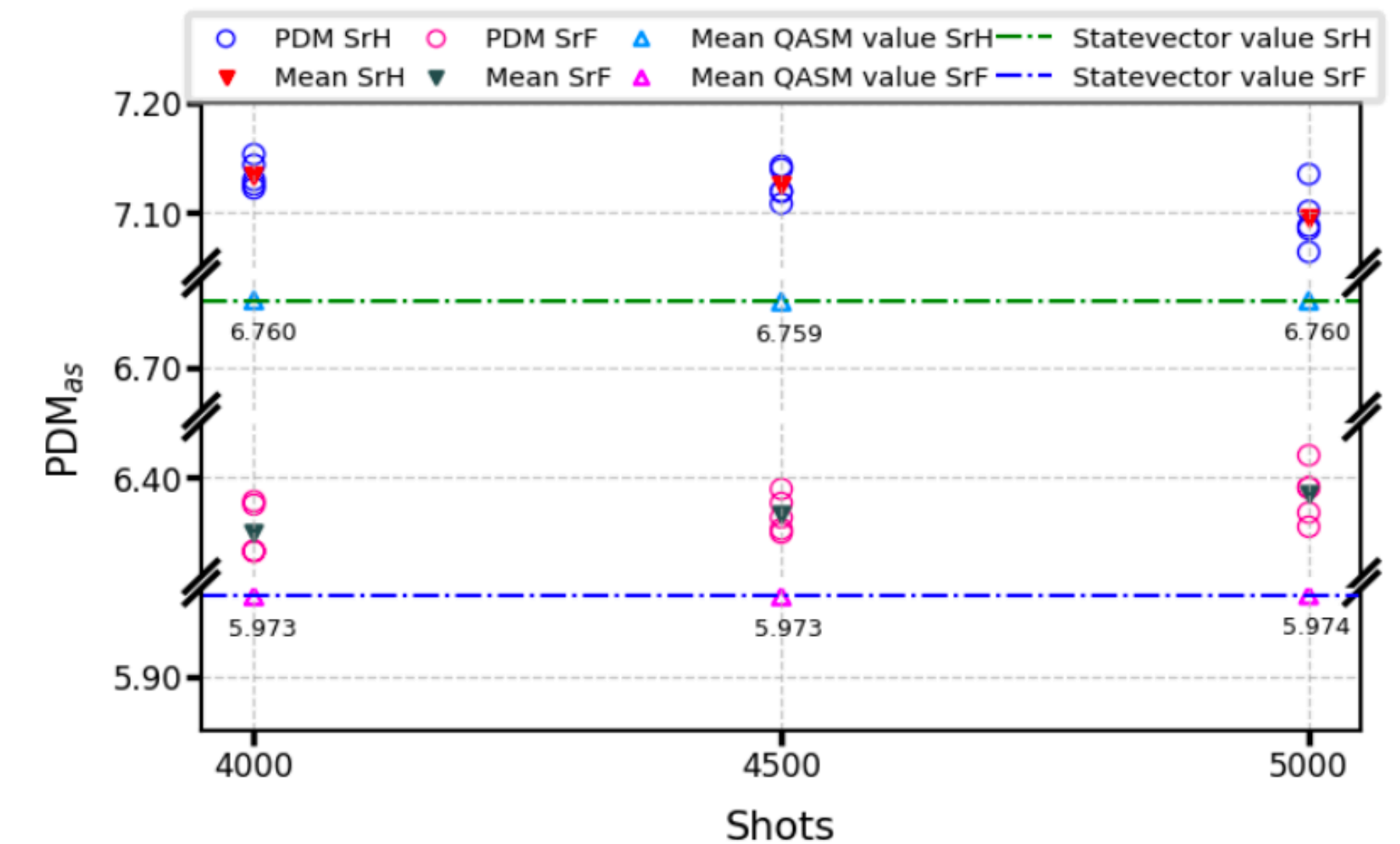
arXiv 2406.04992 (2024)

- Computation of molecular electric dipole moments (PDMs) of **single valence** molecules.
- Choice of ansatz: **unitary coupled cluster** in the singles and doubles approximation (UCCSD): $|\Psi\rangle = e^{T-T^\dagger} |\Phi_0\rangle$; $T = T_1 + T_2$.
- The set of amplitudes $\{t_{ia}, t_{ijab}\} \equiv \{\theta\}$ are the variational parameters.
- **Eighteen qubit simulations**: PDMs of BeH through RaH (3 occupied + 15 unoccupied). Relativistic effects can be as large as 25 percent for PDM of RaH.
- **Six qubit computations on IonQ Aria-I device**: PDMs of moderately heavy SrH and SrF (3+3).
- **Twelve qubit computations on IonQ Forte-I device**: PDMs of moderately heavy SrH (5+7).

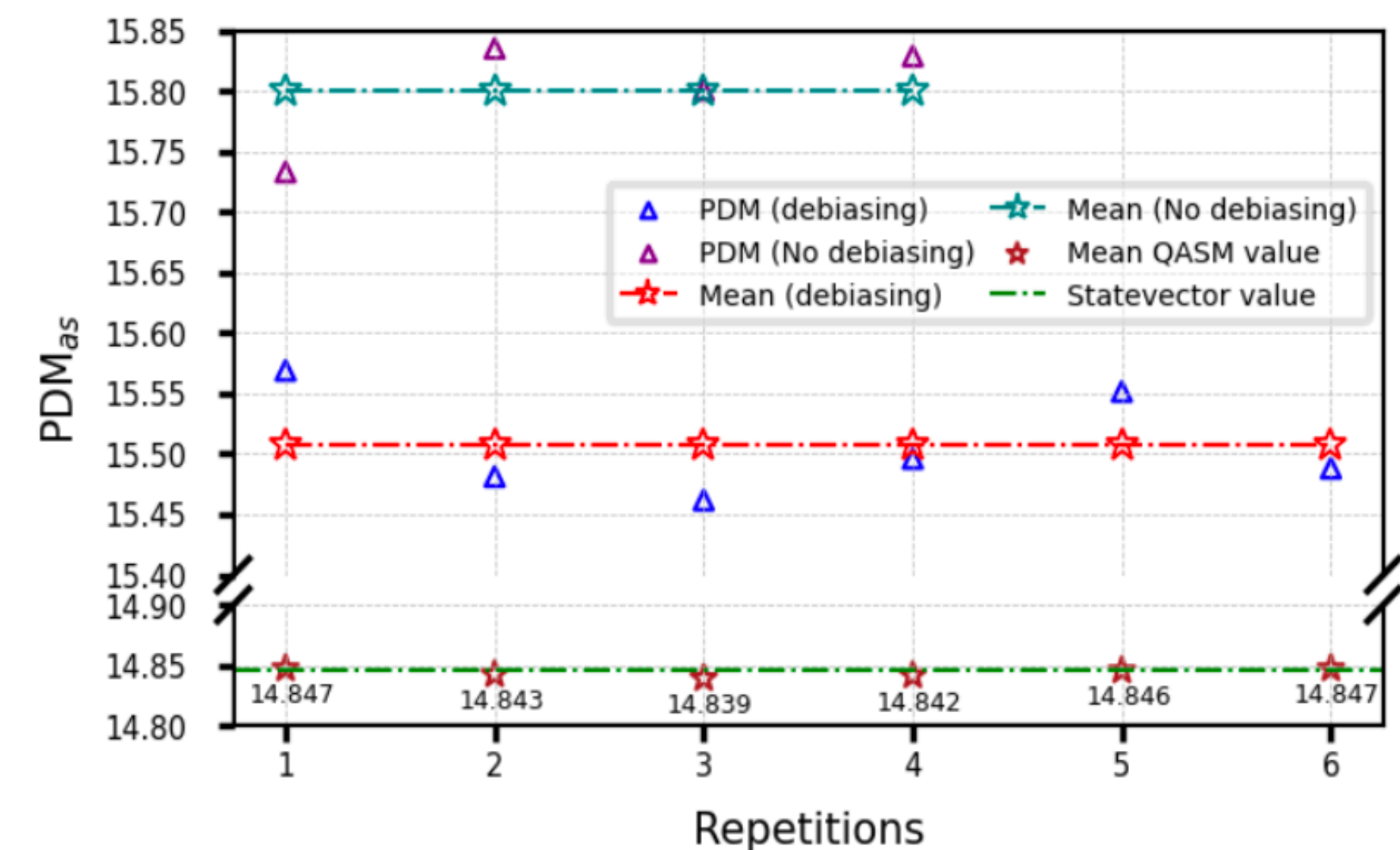
VQE algorithm for relativistic calculations of molecular electric dipole moments

arXiv 2406.04992 (2024)

- For quantum hardware computations, we used a suite of resource reduction strategies: use of point group symmetry, energy sort VQE procedure, pipeline based circuit optimization, RL-based ZX-calculus, cliques to reduce number of terms measured in PDM operator, particle number conserving post selection scheme.
- Six qubit result: Precision of ~5 percent after error mitigation.
- Twelve qubit result: Precision of ~1 percent after error mitigation.



(a)



(b)

Conclusion

- The VQE algorithm has been successfully used for computing ground state properties of lithium-like systems, in particular, ground state energies and hyperfine interactions on superconducting and trapped ion quantum computers have been computed.
- Correct trends for relativistic effects have been reproduced. More qubits are needed for accurate computations of many-body effects.
- For ground state energies, a precision of about 1 percent and for hyperfine structure constants and a precision between 20 and 40 percent has been obtained respectively on a four-qubit superconducting quantum computer at RIKEN.
- For molecular electric dipole moments on IonQ hardware, and obtain ~5 percent and ~1 percent precision for six- and twelve- qubit computations respectively using two different versions of IonQ. The circuit optimisation was superior for the latter case.

QAE algorithm

Quantum annealing

- $\sigma_i^Z |s_i\rangle = s_i |s_i\rangle$. Thus, with $|\Psi\rangle = \otimes_{i=1}^N |s_i\rangle$ as the ground state wave function of the final Hamiltonian, an energy functional

$$\epsilon(s_i) = \langle \Psi | H | \Psi \rangle = \sum_i h_i s_i + \sum_{i,j} J_{ij} s_i s_j.$$

- With $q_i = \frac{s_i + 1}{2}$, we get the QUBO form:

$$\epsilon(q_i)_Q = \sum_i Q_i q_i + \sum_{i,j} Q_{ij} q_i q_j.$$

- The energy functional:

$$\epsilon(c_i) = \frac{\langle \Psi | H | \Psi \rangle}{\langle \Psi | \Psi \rangle} - \lambda \langle \Psi | \Psi \rangle = \sum_i (H_{ii} - \lambda) + \sum_{ij} H_{ij} c_i c_j$$

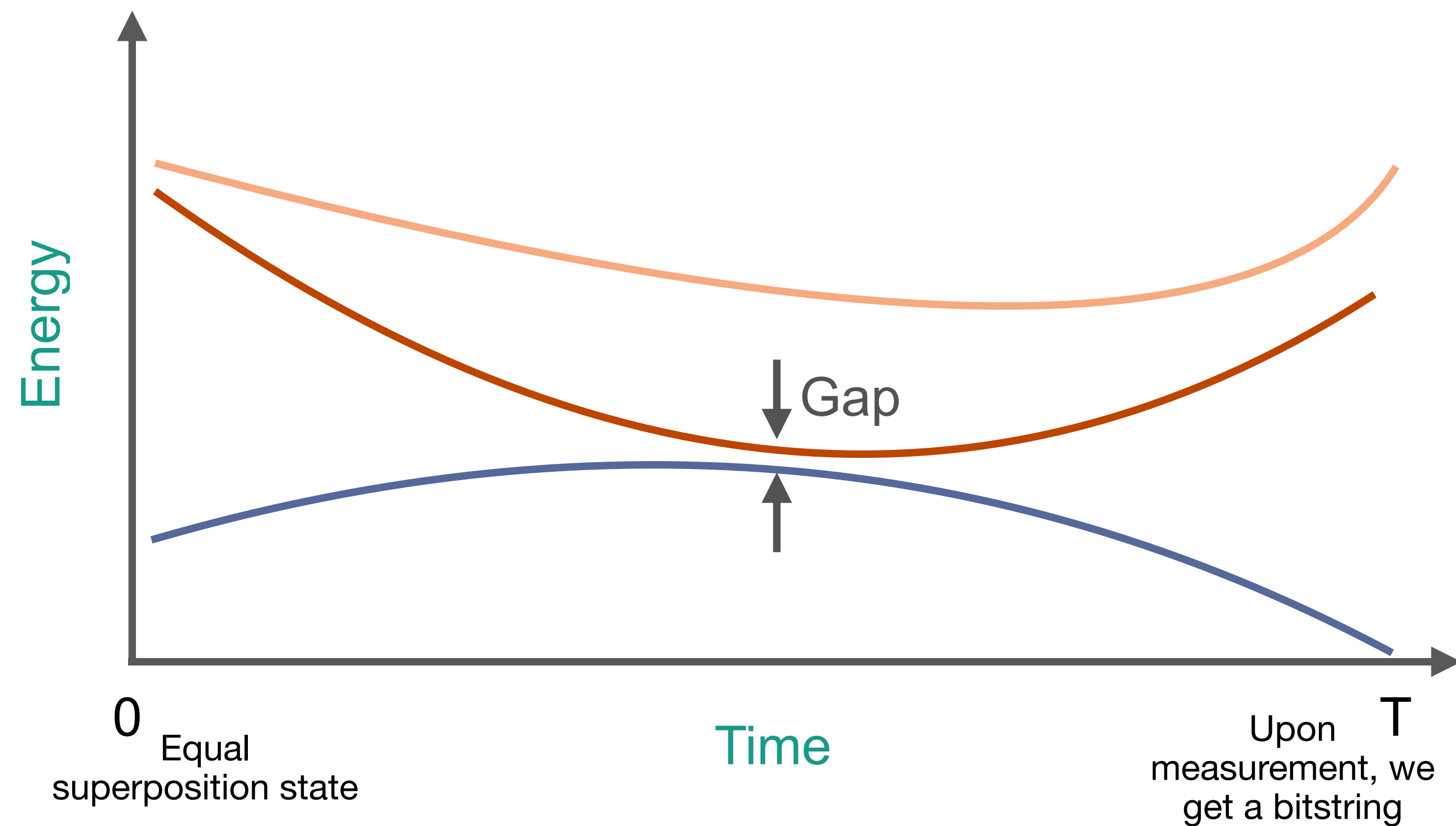
obtained by using $|\Psi\rangle = \sum_i c_i |\Phi_i\rangle$ can be

expressed in QUBO form via a floating point encoding scheme given by

$$c_i^{\{r\}} = c_i^{\{r-1\}} + 2^{\frac{1-r}{2}} \sum_{k=0}^{K-1} f_k 2^{-k} q_k^i.$$

$$H(t) = f(t) \sum_i \sigma_i^x + g(t) H_T \quad \text{Annealing from } 0 \rightarrow T$$

$$H_T = \sum_i h_i \sigma_i^z + \sum_{i<j} J_{ij} \sigma_i^z \sigma_j^z \text{ (Ising)} \quad f(t) : 1 \rightarrow 0, g(t) : 0 \rightarrow 1$$



Initialization

$$H_{DCB} = H_{DC} + H_B$$

Energy functional

$$\epsilon(\lambda, H_{DCB})$$

Final ground state energy

$$\langle \Psi | H_{DCB} | \Psi \rangle$$

Energy

$$\langle \Psi | H_{DCB} | \Psi \rangle$$

Quantum annealer

Construct QUBO functional

$$\epsilon_Q$$

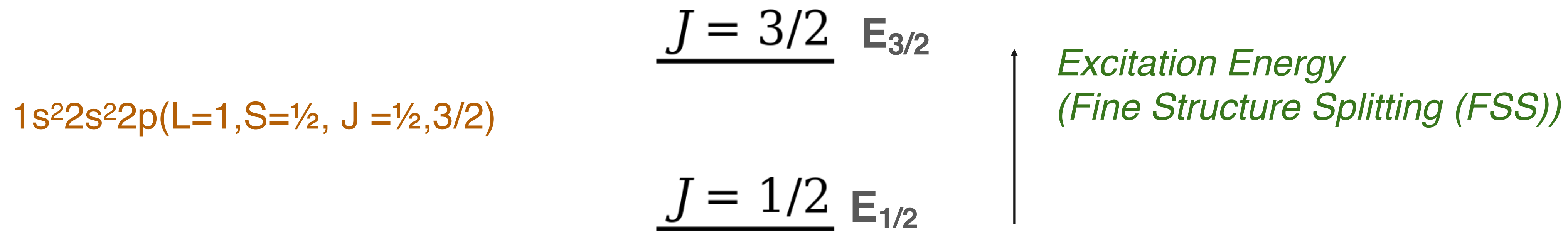
Post-Processing

Construct $|\Psi\rangle$ from qubit configuration

Optimization

D-Wave Advantage 5000Q (Embedding, Annealing)

Computation of Relativistic effects using QAE: Fine structure splitting for Boron-like ions



$$H|\Psi(J = 1/2)\rangle = E_{1/2}|\Psi(J = 1/2)\rangle \quad H|\Psi(J = 3/2)\rangle = E_{3/2}|\Psi(J = 3/2)\rangle$$

**QAE is applied to J=1/2 and J=3/2 states separately
on D-Wave quantum annealer**

Results

FSS values for boron-like ions. ‘relCI’ refers to numerical relativistic CI calculations, ‘Hardware’ gives our mean (over five repetitions) of relativistic QAE performed on the D-Wave Advantage machine. The quantity in bracket is the percentage fraction difference, $\frac{E_{\text{relCI}} - E_{\text{hardware}}}{\text{relCI}} \times 100$. ‘Expt’ stands for the experimental value (in Ha).

System	relCI	Hardware	Expt.
Ca ¹⁵⁺	0.163444	0.163673(-0.1406)	0.166831
Fe ²¹⁺	0.532338	0.532572(-0.0441)	0.538863
Kr ³¹⁺	2.228474	2.228881(-0.0183)	2.244283
Mo ³⁷⁺	4.368104	4.368535(-0.0099)	4.393976

Classical computer

D-Wave quantum
annealer

High precision spectroscopic
measurement

Conclusions and Outlook

- We have performed computations of the Fine Structure Splitting in Boron-like ions using the Quantum Annealer Eigensolver using D-Wave 5000Q.
- We have obtained an accuracy of 99% compared to high precision spectroscopic measurements of the fine structure splitting of these ions.
- The accuracy was achieved by improving the workflow of the QAE algorithm and inclusion of important physical effects.
- This is the first step in carrying out high accuracy quantum annealing computations of atomic quantities that have a wide range of applications including the probing of new physical phenomena beyond the Standard Model of particle physics.

Asides

Hyperfine structure constant

- The **hyperfine Hamiltonian** is given by $H_{hf} = \vec{j}_e \cdot \vec{A}_N$. Thus, $\langle \Psi | H_{hf} | \Psi \rangle = \langle \Psi | \vec{j}_e \cdot \vec{A}_N | \Psi \rangle$.
- The quantity can be rep as an **effective Hamiltonian**: $H_{hf}^{eff} = \mathcal{A} \vec{I} \cdot \vec{J}$, where \mathcal{A} is given by $\mu_I \int \frac{f(r)}{r^3} dV$. μ_I is the nuclear magnetic moment. Thus, $\langle \Psi | H_{hf}^{eff} | \Psi \rangle = \mathcal{A} \langle \Psi | \vec{I} \cdot \vec{J} | \Psi \rangle = \mathcal{A} IJ$.
- $\langle \Psi | H_{hf} | \Psi \rangle = \langle \Psi | H_{hf}^{eff} | \Psi \rangle$. Thus, $\mathcal{A} = \frac{\langle \Psi | H_{hf} | \Psi \rangle}{IJ} = \frac{1}{IJ} \mu_N g_I I \langle JJ | \sum_i \frac{(\vec{r}_i \times \vec{\alpha}_i)_Z}{r_i^3} | JJ \rangle$.
- a is often a hard quantity to evaluate, since it is determined by a complex interplay of several electron correlation effects, unlike the energy.
- Its computation requires accurate single particle wave functions in the nuclear region, and hence computing a is a sensitive test of relativistic and correlation effects in atoms and molecules.

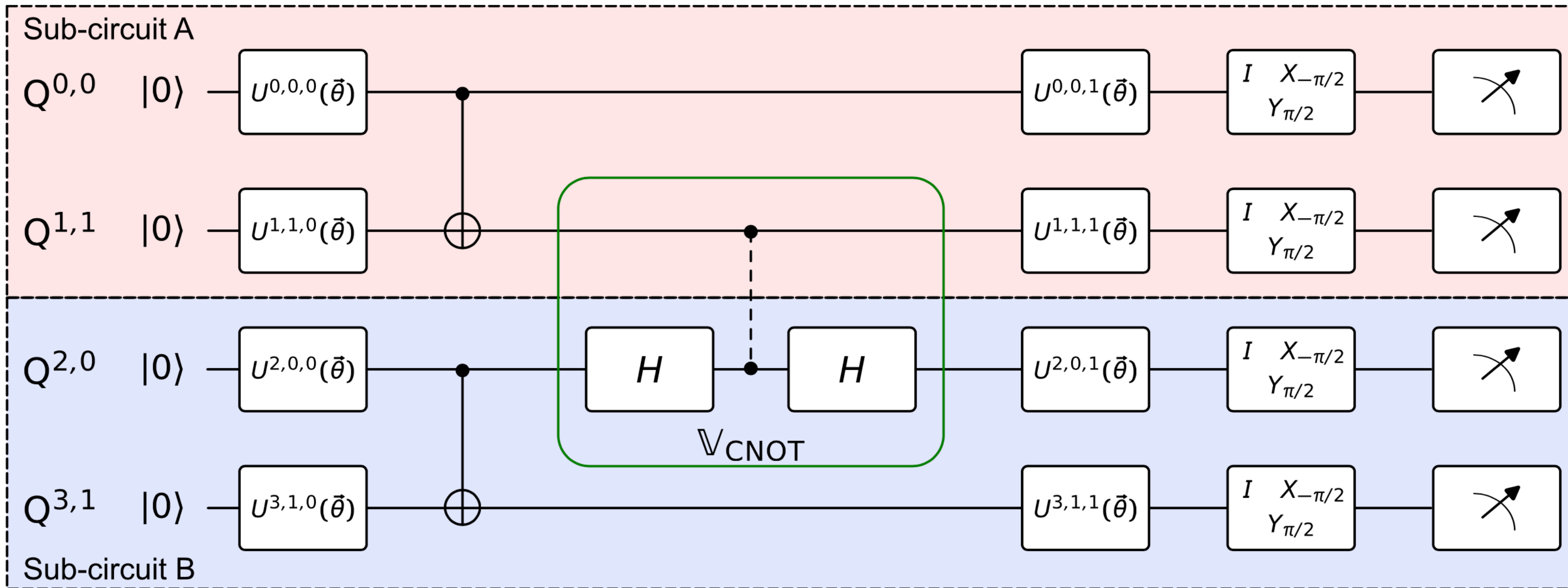


TABLE III: Table presenting the results for ground state energies of the considered systems in the current work (in Hartree). ‘DHF’ refers to the Dirac-Hartree-Fock results, while ‘CAS-CI’ column gives the complete active space configuration interaction results. ‘Experiment’ presents our main results with error bars, and the ‘Spectroscopy’ column presents reference values for comparison. The energies have been rounded off to the sixth decimal place.

System	E^{DHF}	$E^{\text{CAS-CI}}$	E^{exp}
Neutral ${}^7\text{Li}$	-7.4335127217	-7.4335162022	$-7.4543855659503295 \pm 0.0798287484182712$
Li-like ${}^{45}\text{Sc}$	-477.8353626541	-477.8357346180	$-476.94575187918184 \pm 4.936075422739702$
Li-like ${}^{141}\text{Pr}$	-4056.9990824110	-4056.9997468754	$-4065.3785548435794 \pm 41.92837830047333$
Li-like ${}^{209}\text{Bi}$	-8551.2183918008	-8551.2194891481	$-8569.308517928404 \pm 92.42280778719591$

TABLE IV: Table of results for the hyperfine structure constants (in MHz). The notation followed is the same as in the preceding table, Table III. The hyperfine structure constants have been rounded off to the third decimal place.

System	\mathcal{A}^{DHF}	$\mathcal{A}^{\text{CAS-CI}}$	\mathcal{A}^{exp}	$\mathcal{A}^{\text{ref-exp}}$
Neutral ${}^7\text{Li}$	426.467802	433.409404	$402.20317884582784 \pm 200.08846748253467$	4.0175×10^2
Li-like ${}^{45}\text{Sc}$	1242478.818816	1251563.081863	$1426484.2782180058 \pm 129835.77567268706$	1.4992×10^6
Li-like ${}^{141}\text{Pr}$	39700326.835043	39823463.473807	$40505291.717860445 \pm 3471216.2627738793$	4.7513×10^7
Li-like ${}^{209}\text{Bi}$	175245507.394001	175703370.441872	$179222239.0295429 \pm 14002414.502785636$	1.9828×10^8

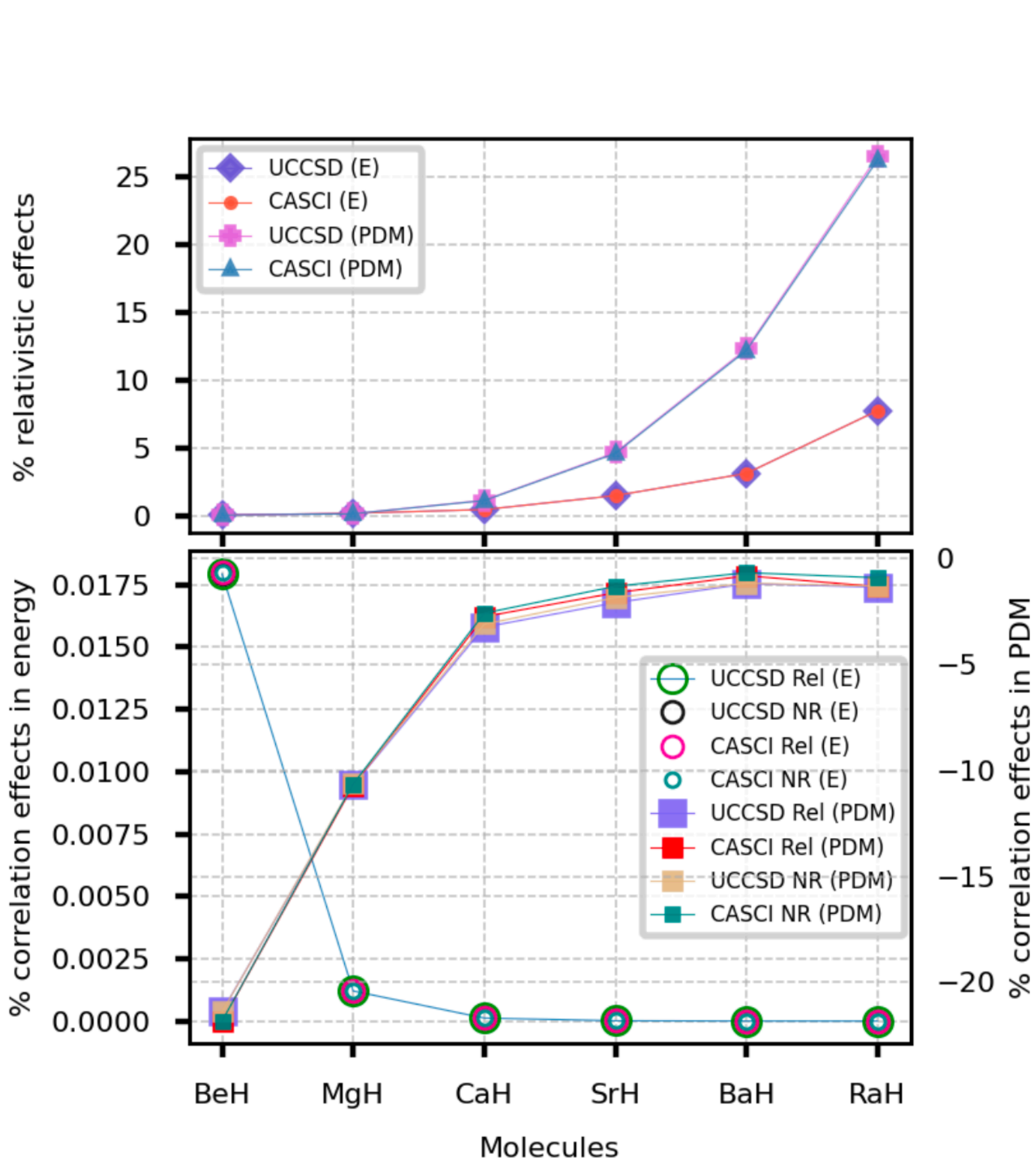


Figure 1. The top panel shows the percentage relativistic effects $= \frac{A_{Rel} - A_{NR}}{A_{Rel}} \times 100$ for ground state energy (E) and PDM from our 18-qubit VQE simulations. Our results are benchmarked against CASCI calculations. The bottom panel shows the percentage correlation effects $= \frac{A_X - A_{MF}}{A_X} \times 100$, where X can be correlation energy (circular markers) or the PDM (square markers) relative to respective quantity at VQE and CASCI levels.

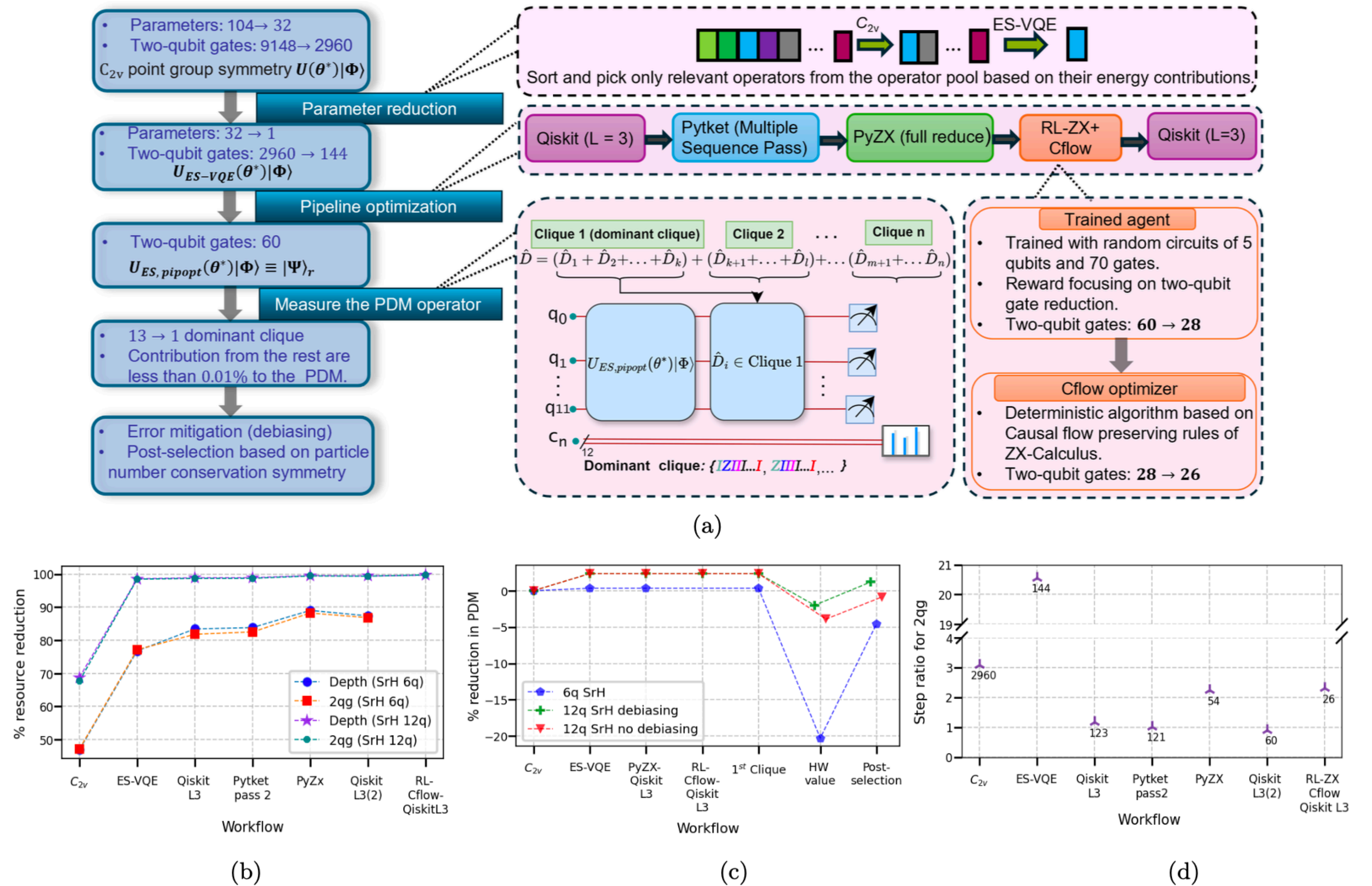


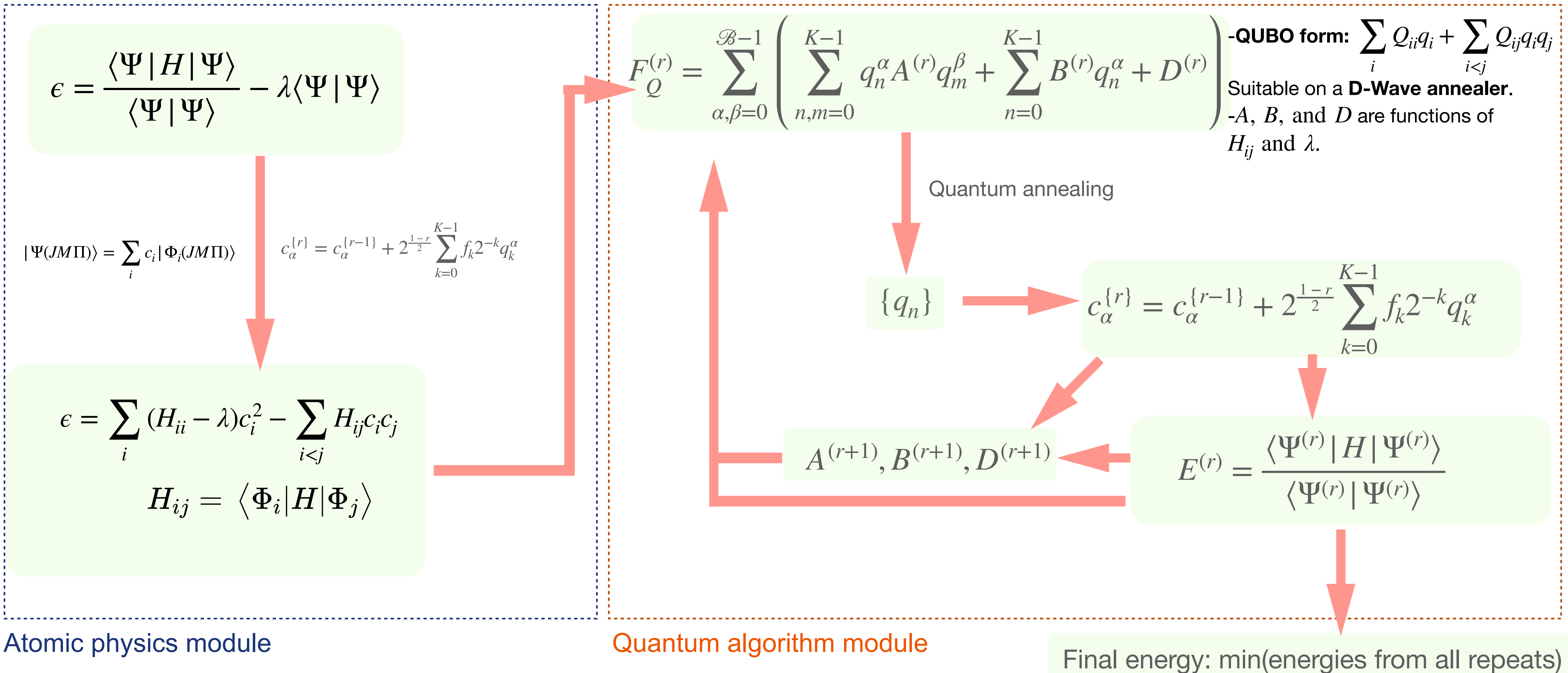
Figure 2. (a) Our workflow for quantum hardware execution of SrH 12-qubit PDM calculation on the IonQ Forte device, which leads to reducing quantum resources while retaining precision. (b) Percentage reduction in resources (two-qubit gates, denoted as $2qg$ in the sub-figure, and circuit depth) with each step of our workflow: U_{ES-VQE} is the UCCSD circuit post-ES-VQE and $U_{ES,Pipopt}$ is the state after pipeline-based optimization (denoted as pipopt). (c) The loss of precision in predicting PDM after each step in our workflow, with '1st Clique' indicating the selection of the dominant clique for the PDM operator (See Table S2 of the Supplemental Material). Sub-figure (d) illustrates the step ratio, which is the ratio of the number of $2qg$ before and after the current step in our workflow. It is important to stress that the compound strategy of our RL-ZX based agent followed by the causal flow deterministic algorithm (both based on ZX-Calculus, denoted as RL-ZX + Cflow) reduces the already small gate count by one half.

QAE: subQUBO

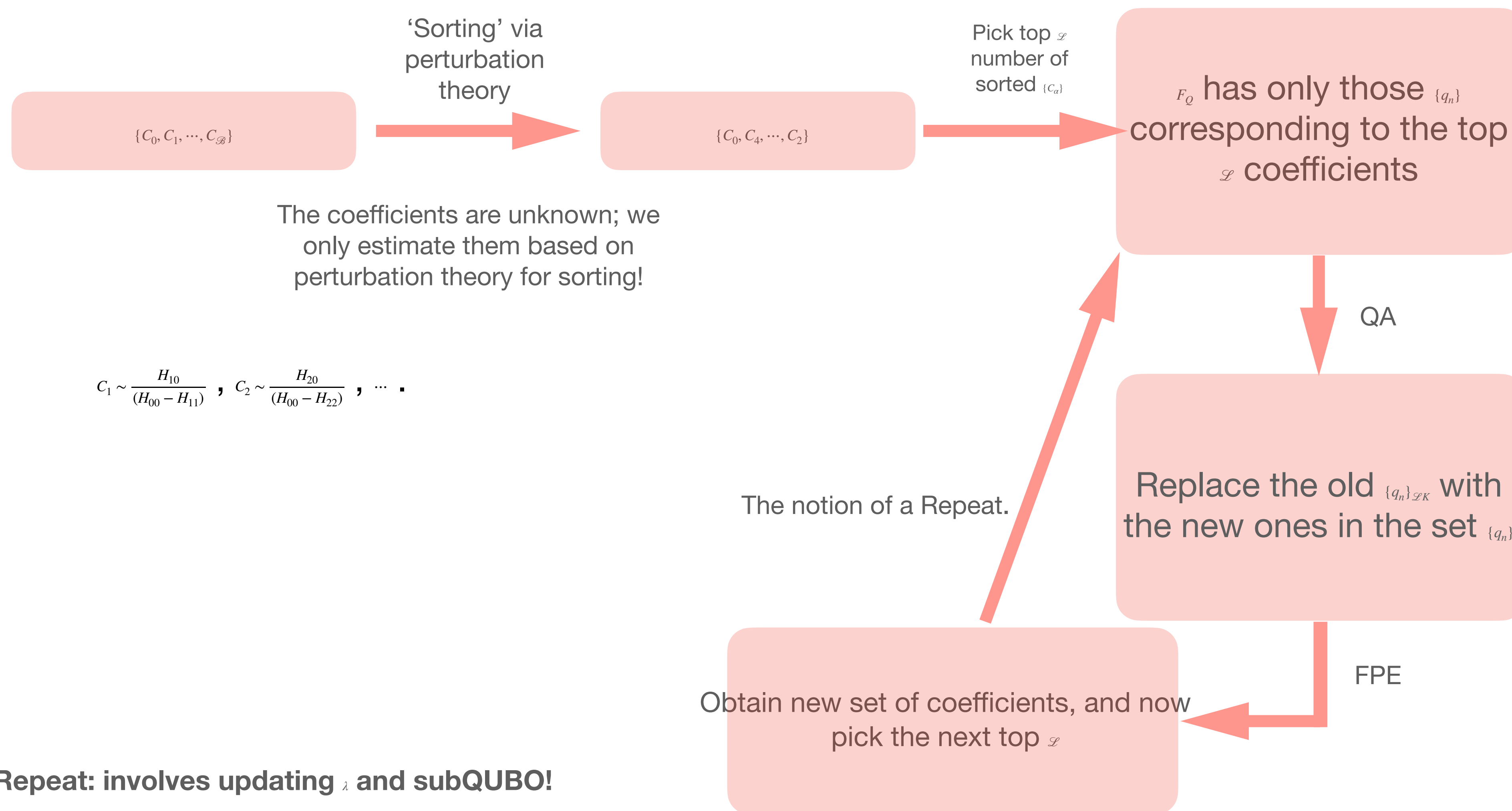


Number of Repeats: 75 (30 for $J=1/2$ and 45 for $J=3/2$), QUBO size: 90 and 160, subQUBO size: 30 (110 qubits) and 40 (190 qubits). Anneal time: 20 microseconds.
Individual energies: Best agreement with relCI: ~ 0.05 mHa, and the worst ~ 1 mHa.

Connection between atomic physics and quantum annealing



subQUBO partitioning and choice



Repeat: involves updating λ and subQUBO!